

Earth's Future

RESEARCH ARTICLE

10.1029/2022EF002655

Special Section:

Advancing flood characterization, modeling, and communication

Multivariate Analysis of Compound Flood Hazard Across Canada's Atlantic, Pacific and Great Lakes Coastal Areas

Farshad Jalili Pirani¹ and Mohammad Reza Najafi¹ 

¹Department of Civil and Environmental Engineering, Western University, London, ON, Canada



Key Points:

- The trivariate joint return periods and failure probabilities are assessed based on vine copula and Bayesian approaches
- Over half of Canada's coastal locations, in particular areas across the Atlantic, are at risk of compound flooding
- Considering the dependencies between multiple flood-generating mechanisms is essential for the robust assessment of flood hazards

Supporting Information:

Supporting Information may be found in the online version of this article.

Correspondence to:

M. R. Najafi,
mnajafi7@uwo.ca

Citation:

Jalili Pirani, F., & Najafi, M. R. (2022). Multivariate analysis of compound flood hazard across Canada's Atlantic, Pacific and Great Lakes coastal areas. *Earth's Future*, 10, e2022EF002655. <https://doi.org/10.1029/2022EF002655>

Received 12 JAN 2022

Accepted 5 JUL 2022

Author Contributions:

Conceptualization: Farshad Jalili Pirani

Data curation: Farshad Jalili Pirani

Formal analysis: Farshad Jalili Pirani

Investigation: Farshad Jalili Pirani

Methodology: Farshad Jalili Pirani

Resources: Farshad Jalili Pirani

Abstract Compound flooding, caused by the simultaneous or successive occurrence of two or more flood mechanisms, is mainly associated with extreme precipitation, river overflows, and storm tides across coastal areas. The interdependencies between these components can increase the risks of flood impacts, threatening coastal communities and infrastructure systems. This study quantifies the corresponding multivariate hazard over Canada's coastal areas by characterizing the dependencies between multiple drivers of flooding based on the C-vine copula statistical approach. The joint return periods of compound flooding considering the AND, OR, and Kendall scenarios are estimated and the corresponding failure probabilities are assessed. Further, the compound hazard ratio (CHR) index is applied to quantify possible under- or overestimations of the flood hazards when individual drivers are assessed independently. Analyses are performed at 41 locations across the Atlantic, Pacific, and the Great Lakes coasts, and the uncertainties are quantified based on the Bayes theorem. Results show that at approximately 50% of locations (mostly at the Great Lakes), the flood hazard associated with the AND scenario increases considerably when the dependencies are characterized compared to the (unrealistic) independence scenario, indicating the potential for compound flooding in these regions. Besides, at more than half of the studied locations, the CHR index exceeds one highlighting the interrelationships between drivers of flooding. The results of this study provide a deeper understanding of the flood mechanisms and their interdependencies across Canada's coasts, which support the development of resilient structures and improved coastal flood management.

Plain Language Summary Approximately half of the global population lives within 200 km of coastlines. The communities and infrastructure systems in the coastal environments are at risk of flooding caused by one or multiple mechanisms. Understanding the compounding effects of the drivers of flooding and quantifying the corresponding uncertainties are critical for flood risk analysis and the development of effective resilience strategies. To address this objective, we investigate compound flood events considering terrestrial (both precipitation, and streamflow which reflects the effects of snow/ice melt in addition to rainfall) and coastal mechanisms across Canada's Atlantic, Pacific and Great Lakes' coasts, with distinct hydroclimate characteristics, based on a state-of-the-art statistical approach. The proposed design flood estimation method addresses the limitations in traditional approaches that neglect the interdependencies between two or multiple drivers of flooding. Further, the proposed approach identifies areas that are at high risk of compound flooding and identifies the main contributing factors. The results suggest that the risk of flooding can increase up to 50% if flood mechanisms are analyzed holistically and the interrelationships are accounted for, compared to estimates from the traditional approach. Precipitation and sea levels are the major factors that contribute to compound flooding, in particular at the Atlantic coast.

1. Introduction

Flooding, as the most common natural hazard in the world (Kundzewicz et al., 2014), has affected more than two billion people and caused approximately USD 656 billion of damage between 1998 and 2017 (AghaKouchak et al., 2020; Wallemaq, 2018). From 1980 to 2019, flood events have accounted for 41% of all the 17,300 weather-related events, 28% of 890,000 lives lost, 27% of USD 4,000 billion economic losses, and 10% of USD 1,300 billion insured losses worldwide (Golnaraghi et al., 2020). The frequency of flood events has been increasing from 1960 to 2013, globally (Tanoue et al., 2016). Similarly, the magnitude of flooding shows increases in some regions around the world (Do et al., 2020). Around 0.8–1.1 million people experience flooding and its devastating socioeconomic consequences each year (Muis et al., 2016), especially the coastal communities. The population of the low-lying coastal areas was approximately 625 million in 2000, which is anticipated to reach 949 million by the 2030s and 1.4 billion by 2060s (Neumann et al., 2015), indicating larger exposure to different

© 2022 The Authors. Earth's Future published by Wiley Periodicals LLC on behalf of American Geophysical Union. This is an open access article under the terms of the [Creative Commons Attribution-NonCommercial-NoDerivs License](https://creativecommons.org/licenses/by/4.0/), which permits use and distribution in any medium, provided the original work is properly cited, the use is non-commercial and no modifications or adaptations are made.

Software: Farshad Jalili Pirani
Validation: Farshad Jalili Pirani
Visualization: Farshad Jalili Pirani
Writing – original draft: Farshad Jalili Pirani
Writing – review & editing: Farshad Jalili Pirani

types of flood hazards in these regions in the future. Therefore, it is critical to understand and predict the mechanisms that drive flooding, including intense rainfall, high seawater levels, and river overflows, as well as their interactions, and interrelationships to develop effective flood mitigation and adaptation strategies.

Conventional approaches to flood hazard assessment are based on the assumption that the drivers of flooding are independent of one another. However, recent studies show strong evidence for the interactions between drivers of floods, especially in coastal areas around the world (Eilander et al., 2020; Hendry et al., 2019; Moftakhari et al., 2017; Nasr et al., 2021; Robins et al., 2021; Wahl et al., 2015; Ward et al., 2018). Different mechanisms can trigger flood events simultaneously or successively, leading to an extreme impact even if the contributing drivers are not extreme (Masson-Delmotte et al., 2021). The physical and socioeconomic consequences of such compound events can be much more drastic compared to the ones associated with the individual drivers (Ward et al., 2018; Zscheischler et al., 2018). Therefore, analyzing different flood types (e.g., fluvial, pluvial, and coastal) in isolation can result in an underestimation of flood risks.

In coastal areas, compound flooding can be associated with low-pressure systems like tropical cyclones that generate strong winds and subsequently storm surges and high waves, along with heavy rainfall and possible river overflows (Couasnon et al., 2019; Paprotny et al., 2018; Svensson & Jones, 2002). Examples of such events include Hurricane Katrina (2005) affecting south Florida (Johnson, 2006), Hurricane Harvey (2017) in south-east Texas (Frame et al., 2020), both with at least \$125 billion in damage, and recent hurricanes of Elsa, and Henri (Eckstein et al., 2021) with \$1.2 billion and \$550 million in damage respectively. Previous studies have analyzed compound flood events at global (Eilander et al., 2020; Ward et al., 2018), continental (Ganguli & Merz, 2019; Paprotny et al., 2020), national (Ghanbari et al., 2021; Jalili Pirani & Najafi, 2020), and regional scales (Valle-Levinson et al., 2020; van Berchum et al., 2020) using statistical and process-based approaches (Hao et al., 2018). These analyses include characterizing the statistical interrelationships between drivers of flooding based on Bayesian networks (Couasnon et al., 2018; Sebastian et al., 2017), copula theory (Bevacqua et al., 2017; Gori et al., 2020; Moftakhari et al., 2017; Paprotny et al., 2018; Xu et al., 2014), bivariate extreme value distributions (Zheng et al., 2014), correlation and linear regression (Robins et al., 2021), bivariate logistic threshold-excess model (Zheng et al., 2013) among others. Besides, recent studies have assessed the compound flood impacts and risks through process-based modeling and hybrid statistical-dynamical framework (Ganguli et al., 2020; Ganguli & Merz, 2019; Najafi et al., 2021; Wang et al., 2021; Zhang & Najafi, 2020).

The theory of copula, introduced to the hydrologic community by De Michele and Salvadori (2003), is commonly applied for the multivariate analysis of flood events as it can represent a wide range of dependence structures between hydroclimatic variables (Singh et al., 2021, 2022). It is a flexible approach for the frequency analysis of compound events that allows for characterizing the individual drivers with the most appropriate distribution functions. The corresponding hazards can be assessed under different scenarios according to the geographic location or the criteria considered for the design, planning, and management of infrastructure systems or coastal communities (a) either of the flood mechanisms is extreme and can affect the study region, for example, the occurrence of an intense rainfall event or storm surge (OR scenario), (b) all the drivers are extremes (AND scenario), and (c) the joint exceedance probability of the drivers is above a certain threshold (Kendall scenario). Using copula models, Ward et al. (2018) studied the global dependencies between high river discharge rates and sea levels, and showed their significant role in the estimated design levels. Bevacqua, Vousdoukas, Zappa, et al. (2020) and Bevacqua, Vousdoukas, Shepherd, et al. (2020) reported an overall 30% increase in the joint probability of extreme meteorological tides and inland precipitation under a high emission scenario along the global coasts by 2100 compared to the present conditions. Ganguli and Merz (2019) showed that for half of the studied locations in northwestern Europe the river discharge rates conditioned on extreme total water levels are higher than the unconditioned rates. Further, Paprotny et al. (2020) found strong dependencies in surge–precipitation and surge–discharge pairs along the northwestern coasts of Europe. Similar analyses have been conducted on the joint occurrence of storm surge and precipitation across coastal zones of China (Fang et al., 2020), Australia (Wu et al., 2018), storm surge, and river discharge in Britain (Robins et al., 2021), storm surge/sea levels and river discharge over the US coasts (Welch, 2020), among others.

Many studies on compound flooding have been focused on the bivariate structure of the driving mechanisms, however, the range of dependencies between multiple factors that can contribute to regional/global flooding is less understood. Liu et al. (2018) investigated the joint occurrence of precipitation and surface runoff in Texas, with the El Niño-Southern Oscillation and rising temperatures as the underlying conditions using vine copula

(also known as pair-copula). Santos et al. (2020) conducted bivariate and trivariate extreme analyses to study the return periods (RPs) of inland water levels as a function of storm surge, tide, and precipitation in the Netherland. Jane et al. (2020) characterized the dependencies between rainfall, sea level, and groundwater level for coastal areas of Miami-Dade County in southeastern Florida. They found that vine copulas could better represent the dependencies between the drivers compared to the symmetric high-dimensional copulas, which consider homogeneity in the type of dependence between each pair of variables and do not account for the conditional dependence between the variables (Aas & Berg, 2009). Vine copula constructs the multidimensional copula without assuming conditional independence (Aas et al., 2009).

Communities and infrastructure systems in Canada's coastal areas, across the Atlantic, Pacific, and the Great Lakes, are at risk of flooding caused by extreme precipitation, river overflows, storm surges, and tides (Bush & Lemmen, 2019; Mahmoudi et al., 2021). Some examples include Hurricane Juan which hit eastern Canada and Nova Scotia resulting in an economic loss of \$200 million in September 2003, Hurricane Dorian in eastern Canada (September 2019) with \$78.9 million in damage, and Hurricane Teddy affecting Nova Scotia in September 2020. Most previous analyses have been focused on the bivariate structure of compound flooding events (e.g., sea level and streamflow or sea level and precipitation). In this study, we analyze multiple drivers of flooding (sea level, precipitation, and streamflow) their interdependencies, and the corresponding joint and conditional return periods across Canada's coasts, for the first time, based on vine copulas. Instead of relying on a limited number of Archimedean (asymmetric) or elliptical (symmetric) copula functions (Beersma & Buishand, 2004; Rana et al., 2017; Shiau, 2006), we consider a comprehensive set of copulas to better represent the extreme dependencies. Bayes theorem is applied to estimate the parameters of the marginal distributions and the copula functions and characterize the uncertainties associated with different hazard scenarios, including AND, OR, and Kendall (dos Santos Silva & Lopes, 2008; Min & Czado, 2011; Pitt et al., 2006; Sarhadi et al., 2016; Smith, 2011). Further, we assess the return levels of flow discharge rates conditioned on precipitation and downstream seawater levels and compare them with the unconditional scenario. We also estimate the failure probabilities (FPs), that is, the possibility of a flood event occurring at least once in a given project's lifetime (Xu, Wang, et al., 2019), corresponding to different hazard scenarios. Besides, for the first time, we provide the trivariate Kendall RP/FP analysis through a sampling technique. Finally, we suggest the optimum design levels of the three drivers considering the corresponding interdependencies.

The remainder of this article is as follows. Section 2 describes the study area and data. The copula and Bayes approaches are presented in Section 3 followed by the discussion of results in Section 4 and the concluding remarks in Section 5.

2. Study Area and Data

Canada has the longest coastline (approximately 230,000 km) worldwide settling over seven million people. We assess compound flooding across its three main domains of the Pacific, Atlantic, and the Great Lakes coasts (Figure 1) by investigating the interactions between Precipitation (Pr; daily time scale), Streamflow (Q; daily), and Total Water Level at the coastal zones (TWL; hourly). The corresponding data at each location are selected for 1960 to 2015 according to the following criteria: each year having more than 20% missing data is removed for each tidal gauge, followed by removing gauges with more than 20% missing data over the entire period. Precipitation and streamflow gauges that lie within a radius of 0.5° (almost 55 km) from each tidal gauge are identified followed by the application of the first two selection steps. In addition to the physical distance of streamflow gauges, flow routes are tracked to make sure they are directed toward the oceans/lakes (Ward et al., 2018). At all locations, extreme sea levels are represented by the maximum hourly TWL at each 24-hr interval.

In cases where several precipitation or streamflow gauges exist within the specified radius, the closest and most downstream ones are selected, respectively. If no hydroclimatic gauges exist within this distance, the radius is increased to a maximum of 100 km to identify at least one precipitation and one streamflow gauge (Wu et al., 2018). The choice of the distance is to ensure that gauge data are representative of the homogeneous hydroclimatic conditions of their locations (Ward et al., 2018). The average distance between the paired streamflow/tide gauges is 59.2 km with a 95% range of 16.8–94.7 km. The corresponding values for the paired precipitation/tide gauges, and streamflow/precipitation gauges are 34.1 km (4.5–97.6 km) and 65.3 km (14.5–93.3 km), respectively. Forty-one locations having more than 80% overlap between TWL, precipitation, and streamflow data

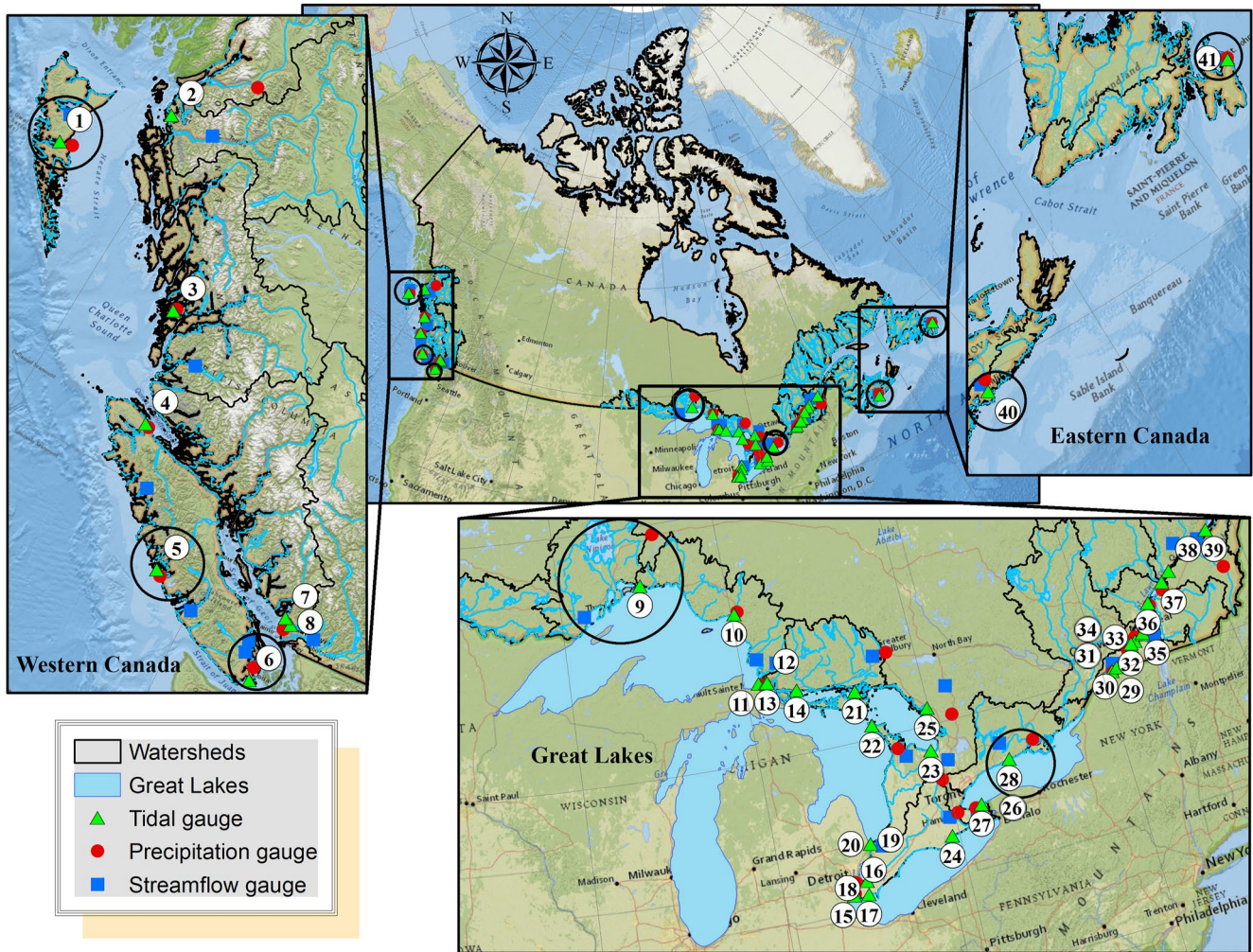


Figure 1. The study area and the locations of precipitation, streamflow, and tidal gauges across the Atlantic, Pacific, and the Great Lakes coasts. Circles show examples of three gauges that are grouped together for multivariate analysis.

records are retained. The names of these locations are provided in Table S3 in Supporting Information S1. Further information is provided in Jalili Pirani and Najafi (2020).

3. Methodology

The simultaneous occurrence of multiple drivers of flooding, including extreme Pr, TWL, and/or Q, is relatively rare, however, the corresponding impacts can be catastrophic (Fang et al., 2020; Wahl et al., 2015). Such disasters can be associated with hurricanes striking coastal areas, especially in small, impervious, round-shape watersheds with a rapid hydrologic response. Besides, coastal flooding due to extreme waves and storm surges superimposed on high tides can be exacerbated by moderate or even low rainfall events. Furthermore, above normal sea levels can block the river system drainage, which combined with high precipitation rates can lead to severe flood impacts in coastal zones. Similarly, simultaneous extreme discharge rates and low/moderate Pr and TWLs can lead to compound flood events threatening coastal communities and infrastructure.

In this study, we analyze compound flooding caused by extreme precipitation events and maximum TWL and Q within ± 1 day of the corresponding event. Extreme events are commonly identified based on the annual maxima of the data records or exceedances above high thresholds (Bezak et al., 2014; Dodangh et al., 2019; Villarini et al., 2011). We consider the peaks over threshold (POT) approach such that the $(Pr_{0.95}, TWL1, Q1)$ scenario represents the joint occurrence of extreme precipitation events exceeding the 95th percentile, and TWL1/Q1

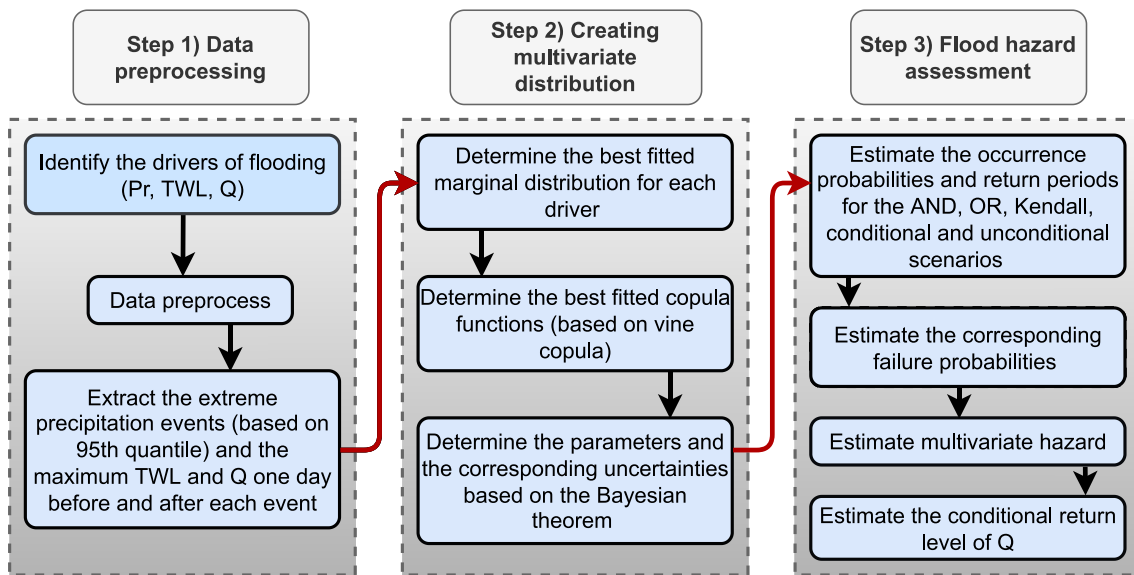


Figure 2. Statistical analysis of compound flooding; Pr, TWL, and Q denote precipitation, total water level, and streamflow, respectively.

which represents the maximum total water levels and flow discharge rates within a 1-day window of precipitation extreme events, respectively. To remove temporal dependencies in extreme precipitation events, only the peaks of 3-day intervals are retained.

The overall procedure for compound flood analysis is summarized in a flowchart (Figure 2) and illustrated in the following sections.

3.1. Copula

The joint variability of the three drivers of flooding across Canada's coasts is characterized based on copula (Joe, 1997; Nelson, 1998). Copula functions (Sklar, 1959) can represent the multivariate behavior of random variables and characterize the corresponding dependence structure (linear, non-linear, tail dependence) (Genest & Favre, 2007). According to Sklar's theorem, if X_1, X_2, \dots, X_n are n continuous random variables, there exists a unique copula C on $(0,1)^d$ that can describe the corresponding joint cumulative distribution function (CDF):

$$F(X_1, \dots, X_n) = C(F_1(X_1|\theta_1), F_2(X_2|\theta_2), \dots, F_n(X_n|\theta_n) | \theta_c) \quad (1)$$

where d is the dimension, $F(X_1, \dots, X_n)$ is the joint CDF of X_1, X_2, \dots, X_n , C is the copula function with the dependence parameter θ_c , $F_1(X_1|\theta_1), F_2(X_2|\theta_2), \dots, F_n(X_n|\theta_n)$ are the marginal distributions with parameters θ_1 to θ_n , respectively. The practical implication of Sklar's theorem is that modeling the marginal distributions can be conveniently separated from the dependence modeling using copula (Brechmann & Schepsmeier, 2013). The corresponding joint probability density function is:

$$f(X_1, \dots, X_n) = \left(\prod_{i=1}^n f_i(X_i) \right) \times c(F_1(X_1|\theta_1), F_2(X_2|\theta_2), \dots, F_n(X_n|\theta_n) | \theta_c) \quad (2)$$

where c is the copula density function.

Initial analysis of the dependencies is performed using the nonparametric Kendall's Tau correlation metric, which measures the degree of association between two variables (Text S1 in Supporting Information S1).

- Vine Copula

We consider the vine copula, introduced by Joe (1996) and further developed by Bedford and Cooke (2001, 2002), for the multivariate analysis of compound flooding. Vine copula can determine the different dependence structures

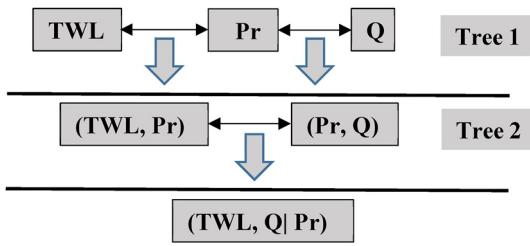


Figure 3. Three-dimensional C-vine copula considering three drivers of flooding (TWL, Pr, and Q).

between multiple variables and is not bound by parameter restrictions when the number of variables increases (Aas & Berg, 2009; Jane et al., 2020; Liu et al., 2018).

Vine copula creates n -dimensional multivariate distributions using a cascade of $n(n - 1)/2$ bivariate or conditional bivariate copulas that are independent of each other. The so-called pair-copulas are flexible in characterizing the dependence structure of multiple variables including the tail dependencies and asymmetries. Bedford and Cooke (2001, 2002) proposed a systemized procedure called regular vine, with two special subclasses of the canonical (C-vine) and drawable vines (D-vine), to decompose a multivariate probability in s the form of a nested set of trees (Text S2 and Figure S1 in Supporting Information S1).

Considering the three drivers of TWL, Pr, and Q, first, the pair-copulas (TWL, Pr) and (Pr, Q) are created at tree 1 and then the conditional copula (TWL, Q | Pr) is determined at tree 2, according to C-vine (Figure 3).

The n -dimensional density function of the C-vine copula is expressed as follows (Brechmann & Schepsmeier, 2013; Czado, 2010):

$$f(X_1, \dots, X_n) = \prod_{k=1}^n f_k(X_k) \times \prod_{i=1}^{n-1} \prod_{j=1}^{n-i} c_{i,i+j|1:(i-1)}(F(X_i|X_1, \dots, X_{i-1}), F(X_{i+j}|X_1, \dots, X_{i-1})) \quad (3)$$

where $f(X_1, \dots, X_n)$ is the joint probability density function of n random variables, $f(X_k)$, $k = 1, \dots, n$, denotes the marginal probability densities, and $c_{i,i+j|1:(i-1)}$ represents the bivariate copula densities with parameter(s) $\theta_{i,i+j|1:(i-1)}$. According to Equation 3, the three-dimensional probability density of the C-vine copula model is expressed as:

$$\begin{aligned} f(Pr, TWL, Q) &= f(Pr) \times f(TWL) \times f(Q) && \text{(marginals)} \\ &\times c_{Pr,TWL}(F(Pr), F(TWL)|\theta_{c(Pr,TWL)}) \times c_{Pr,Q}(F(Pr), F(Q)|\theta_{c(Pr,Q)}) && \text{(unconditional pairs)} \\ &\times c_{TWL,Q|Pr}(F(TWL|Pr), F(Q|Pr)|\theta_{c(TWL,Q)}) && \text{(conditional pair)} \end{aligned} \quad (4)$$

where $f(Pr, TWL, Q)$ is the joint probability density of Pr, TWL, and Q; $f(Pr)$, $f(TWL)$, $f(Q)$ are the corresponding marginal distributions; $c_{Pr,TWL}$, $c_{Pr,Q}$ and $c_{TWL,Q|Pr}$ are the copula functions that characterize the dependencies between Pr and TWL, Pr and Q, and TWL and Q conditioned on Pr, respectively. $\theta_{c(Pr,TWL)}$, $\theta_{c(Pr,Q)}$ and $\theta_{c(TWL,Q)}$ are the corresponding copula parameters associated with (Pr, TWL), (Pr, Q), and (TWL, Q), respectively. The parameters of the marginal distributions θ_m are estimated using the maximum likelihood method. The best-fitted distributions of Q and TWL are selected among normal, lognormal, gamma, Gumbel, exponential, generalized extreme value (GEV), generalized pareto distribution (GPD), Weibull, logistic, and Cauchy distributions (Table S1 in Supporting Information S1) based on the Akaike Information Criterion (AIC) (Akaike, 1974). AIC is defined as:

$$AIC = 2k - 2\ln(L) \quad (5)$$

where k is the number of parameters and L represents the maximum value of the likelihood function for the model. The Kolmogorov-Smirnov (KS) goodness-of-fit test is also applied to verify the best-fitted distribution considering a significance level of 0.05 (Chakravarty et al., 1967). Extreme precipitation events are represented by the GPD with parameters $\theta_m = (\mu, \sigma, \xi)$.

The (un)conditional one- or two-parameter (θ_c) copulas (Schepsmeier et al., 2015) are selected from 41 functions including Gaussian, Student t, Frank, Joe, Clayton, Gumbel, BB1, BB6, BB7, BB8, Tawn type 1, and Tawn type 2 along with their rotational variants (90, 180, and 360°) (Table S2 in Supporting Information S1). The best-fitted copula function is selected based on AIC. Besides, a goodness-of-fit test proposed by Genest et al. (2006) is applied to evaluate the selected model, considering that AIC would select one model with the best relative score even if all models are “wrong” (Burnham et al., 2010; Singh et al., 2020) (Text S3 in Supporting Information S1). The parameters of the marginal distributions and the copula functions, corresponding to (Pr, TWL), (Pr, Q), and (Q, TWL|Pr), is inferred based on the Bayesian approach, and the uncertainties in return periods (RPs) and return levels are quantified (Text S4 in Supporting Information S1).

3.2. Hazard Analysis

- Estimating the joint return period (JRP)

Assessing the hazard associated with individual and compound flood events is critical for water resources planning and management. We estimate the JRPs of multiple flood drivers considering OR (at least one driver exceeds a threshold), AND (all drivers are above specific thresholds), and Kendall (the joint probabilities exceed defined thresholds) scenarios (G Salvadori & De Michele, 2004; Salvadori et al., 2007; Shiau, 2006). Considering pr , q , and twl as levels beyond which pluvial, fluvial, or coastal flooding can occur, respectively, the exceedance probability and the corresponding return period of the OR scenario are estimated by:

$$P_{OR} = P((Pr > pr) \cup (Q > q) \cup (TWL > twl)) = 1 - C(F_{Pr}(pr|\theta_{mp}), F_Q(q|\theta_{mq}), F_{TWL}(twl|\theta_{mtwl})|\theta_c) \quad (6)$$

$$JRP_{OR} = \frac{\mu}{P_{OR}} \quad (7)$$

where P_{OR} is the probability that at least one of the drivers exceeds the specified threshold (either pr , q , or twl). θ_{mpr} , θ_{mq} and θ_{mtwl} are the set of parameters corresponding to the marginal distributions of Pr, Q, and TWL, respectively. C is the joint cumulative probability of the three drivers of flooding obtained by integrating Equation 4. θ_c is the set of parameters corresponding to the pair-copulas $C_{Pr,TWL}(F(Pr), F(TWL))$, $C_{Pr,Q}(F(Pr), F(Q))$, or $C_{TWL,Q|Pr}(F(TWL|Pr), F(Q|Pr))$, and μ is the average interarrival time between the flood events (in an annual time scale), which is obtained through summing the sequential time intervals between the events divided by $365*(n - 1)$ and n is the number of events.

The worst-case scenario constitutes the simultaneous occurrence of multiple extreme events (i.e., joint occurrence of heavy precipitation, high river flows, and high water levels) that can lead to more severe hazard conditions. This joint probability (AND) and the corresponding JRP are obtained by:

$$\begin{aligned} P_{AND} = P((Pr > pr) \cap (Q > q) \cap (TWL > twl)) = & 1 - F_{Pr}(pr|\theta_{mp}) - F_Q(q|\theta_{mq}) - F_{TWL}(twl|\theta_{mtwl}) \\ & + C_{Pr,TWL}(F(Pr), F(TWL)|\theta_{c(pr,twl)}) + C_{Pr,Q}(F(Pr), F(Q)|\theta_{c(pr,q)}) \\ & + C_{TWL,Q|Pr}(F(TWL|Pr), F(Q|Pr)|\theta_{c(twl,q)}) - C(F_{Pr}(pr|\theta_{mp}), F_Q(q|\theta_{mq}), F_{TWL}(twl|\theta_{mtwl})|\theta_c) \end{aligned} \quad (8)$$

$$JRP_{AND} = \frac{\mu}{P_{AND}} \quad (9)$$

where P_{AND} is the AND probability of the three drivers exceeding their corresponding thresholds (pr , q , or twl). $F_{Pr}(pr|\theta_{mp})$, $F_Q(q|\theta_{mq})$, and $F_{TWL}(twl|\theta_{mtwl})$ are the marginal probabilities of Pr, Q, and TWL given their set of parameters θ_{mpr} , θ_{mq} , and θ_{mtwl} , respectively. $C_{Pr,TWL}(F(Pr), F(TWL)|\theta_{c(pr,twl)})$, $C_{Pr,Q}(F(Pr), F(Q)|\theta_{c(pr,q)})$, and $C_{TWL,Q|Pr}(F(TWL|Pr), F(Q|Pr)|\theta_{c(twl,q)})$ are the bivariate unconditional or conditional copula functions given the corresponding set of parameters θ_c . In this study, the JRPs of both scenarios (AND, OR) are estimated at all locations considering an exceedance probability of 0.01 and compared with the ones associated with the traditional approach (i.e., assuming independence between the drivers of flooding) and with the univariate RP of the individual drivers.

Previous studies (e.g., Salvadori et al., 2011, 2016 and Xu, Wang, et al., 2019) suggest that the OR and AND scenarios might not identify all the dangerous regions in the probability space that can result in under- or over-estimations of the engineering designs. Salvadori and De Michele (2010) proposed Kendall's approach, which is based on the Kendall distribution function. However, the Kendall scenario does not have a direct physical/structural interpretation and can be used for preliminary hazard assessments (Salvadori et al., 2016). Accordingly, the probability space is divided into three zones, a critical probability layer p (a line in the 2D and a surface in the 3D probability space), a dangerous region denoted as S_p^d (d denotes dangerous region) that includes all the events with the joint probabilities more than p , a safe region denoted as S_p^s (s denotes safe region) including the events with joint probabilities less than p (Salvadori et al., 2016). The JRP of the dangerous region is defined as

$$JRP_{Kendall} = \frac{\mu}{P[C(F_{Pr}(pr|\theta_{mp}), F_Q(q|\theta_{mq}), F_{TWL}(twl|\theta_{mtwl})|\theta_c) > p]} = \frac{\mu}{1 - K_c(p)} \quad (10)$$

where $K_c(p) = P[C(F_{Pr}(pr|\theta_{mp}), F_Q(q|\theta_{mq}), F_{TWL}(twl|\theta_{mtwl})|\theta_c) \leq p]$. Estimation of $K_c(p)$ for trivariate analysis of compound flood drivers can be complex. In this study, we resample Pr, Q, and TWL n times using the generated joint probability distribution and assess the corresponding joint probabilities. And the critical layer is obtained considering the 0.01 exceedances for marginals. And the number of events out of n with probabilities lower than the critical layer is divided by the sample size (n) to derive $K_c(p)$.

- Compound hazard ratio (CHR)

Ganguli and Merz (2019) proposed the CHR index to characterize the interactions between different drivers and their effects on the return level estimates of compound events. This index is the ratio between the conditional T-year flow discharge rate considering the annual maximum TWL as the covariate and the unconditional T-year discharge. In other words, the index is calculated by dividing the return level of streamflow conditional on annual max TWL by its univariate (unconditional) return level. We extend this index for trivariate analysis of compound flooding and estimate the ratio of conditional and unconditional streamflow. The probability of T-year Q given Pr and TWL, denoted as Q'_T , is obtained according to Gonzalez-Lopez et al. (2019):

$$P(Q \leq q | Pr \leq pr, TWL \leq twl) = \frac{P(Q \leq q, Pr \leq pr, TWL \leq twl)}{P(Pr \leq pr, TWL \leq twl)} \quad (11)$$

$$= \frac{C(F_Q(q|\theta_{mq}), F_{Pr}(pr|\theta_{mpr}), F_{TWL}(twl|\theta_{mtwl})|\theta_c)}{C(F_{Pr}(pr|\theta_{mp}), F_{TWL}(twl|\theta_{mtwl})|\theta_c)}$$

The CHR index is:

$$CHR = \frac{Q'_T}{Q_T} = \frac{C_{Q|(Pr=pr, TWL=twl)}^{-1} \left[1 - \frac{\mu}{T_{Q|(Pr, TWL)}(q|pr, twl)} \right]}{F_Q^{-1} \left[1 - \frac{\mu}{T_Q(q)} \right]} \quad (12)$$

Q'_T and Q_T are the conditional and unconditional return levels of Q. In this study, the levels of p for the three drivers correspond to a return period of 100 years $C_{Q|(Pr=pr, TWL=twl)}^{-1}$ and F_Q^{-1} are the inverse quantile transformations of copula-based and marginal distributions, respectively. $T_Q(q)$ is the T-year unconditional RP of streamflow $T_Q(q) = \frac{\mu}{1-F_Q(q|\theta_{mq})}$, and the conditional RP of streamflow $T_{Q|(Pr, TWL)}(q|pr, twl)$ is calculated as:

$$T_{Q|(Pr, TWL)}(q|pr, twl) = \frac{\mu}{1 - P(Q \leq q | Pr \leq pr, TWL \leq twl)} \quad (13)$$

- Failure probability

The hydrologic risk is assessed based on the failure probability (FP), which refers to the probability of a flood event that occurs at least once during a given project lifetime (Xu, Wang, et al., 2019). The failure probability is obtained from:

$$FP = 1 - \prod_{i=1}^N F(Pr_i, Q_i, TWL_i) \quad (14)$$

F represents the non-exceedance probability, and N is the number of events during the project lifetime (D) which is inversely related to the average interarrival time between the events (μ):

$$N = \frac{D}{\mu} \quad (15)$$

In this study, we assess FPs corresponding to the AND, OR, Kendall, independence, and univariate scenarios for return periods of 100 and 10 years and lifetimes ranging from 1 to 50 years. Further, the trivariate hydrologic risk for each driver considering the 100-year RP of the other two drivers was quantified.

According to Equation 14, in the OR scenario:

$$FP_{OR} = 1 - \prod_{i=1}^N C(F_{Pr_i}(pr|\theta_{mp}), F_{Q_i}(q|\theta_{mq}), F_{TWL_i}(twl|\theta_{mtwl})|\theta_c) \quad (16)$$

In the AND scenario:

$$\begin{aligned}
 FP_{AND} = & 1 - \prod_{i=1}^N (F_{Pr_i}(pr|\theta_{mp}) + F_{Q_i}(q|\theta_{mq}) + F_{TWL_i}(twl|\theta_{mtwl})) \\
 & + C_{Pr,TWL}(F(Pr), F(TWL)|\theta_{c(pr,twl)}) - C_{Pr,Q}(F(Pr), F(Q)|\theta_{c(pr,q)}) - C_{TWL,Q|Pr}(F(TWL|Pr), F(Q|Pr)|\theta_{c(twl,q)}) \\
 & + C(F_{Pr}(pr|\theta_{mpr}), F_{Q}(q|\theta_{mq}), F_{TWL}(twl|\theta_{mtwl})|\theta_c)
 \end{aligned} \tag{17}$$

And, in the Kendall scenario:

$$FP_{Kendall} = 1 - \prod_{i=1}^N K_c^i(p) \tag{18}$$

4. Results and Discussion

4.1. Marginal Distributions and Pair-Copula Functions

The best-fitted distribution representing each driver of flooding at each location is selected from 10 parametric distributions based on the AIC criterion. Further, the KS goodness of fit test is applied to verify the selected distributions, which are shown in Table S3 in Supporting Information S1 along with the corresponding AIC and p -values. In most locations, the river discharge rates (Q) are represented by GPD and exponential distributions, and the total water levels (TWL) by GPD and Weibull distributions. As discussed in Section 3, extreme precipitation amounts follow GPD at all locations.

The pair-copulas, of the C-vine model, are selected from 41 copula functions based on AIC at each location. According to Equation 4, three pair-copulas (two unconditional and one conditional) are determined to assess the corresponding compound flood hazards (Table S4 in Supporting Information S1). The results show that overall, the majority of the joint variations follow the Frank copula function. The analyses of the bivariate dependencies based on Kendall's tau show that the dependencies between (Pr, TWL) are mostly positive and significant across all locations, especially the Atlantic and Pacific coasts. Pr and Q show positive dependencies in fewer locations compared with (Pr, TWL), especially at the Great Lakes and Pacific regions. Moreover, the joint (Q, TWL) event indicates positive dependencies over both coasts and mostly eastern GL. The number of locations out of 41 with significant dependencies for (Pr, TWL), (Pr, Q), (Q, TWL) is 31 (7 at the Pacific, 22 at the Great Lakes, and 2 at the Atlantic area), 32 (4 at Pacific coast, 27 at Great Lakes, and 1 at Atlantic coast), and 33 (7 at Pacific coast, 24 at Great Lakes and 2 at Atlantic coast), respectively (Table S5 in Supporting Information S1, Figure 4). Besides, there are 13 locations mainly at the Pacific and GL area where the three joints show positive dependencies. However, more sites with positive dependencies are found at three regions regarding the bivariate events of (Pr, TWL) and (Q, TWL). The dependencies between Pr/TWL are stronger (from 0.4 at the Pacific to 0.02 at the GL) than Pr/Q and Q/TWL in the majority of the locations across the three domains (Figure S3 in Supporting Information S1). This can be partly associated with the occurrence of seiche events combined with intense rainfall in the coastal areas at the GL and the extratropical cyclones striking the coasts, especially the Atlantic. Besides, extreme flows depend on several basin characteristics. For example, steep basins with a quick hydrological response, high mean elevation, compacted soil, and impermeable bedrocks are found on the west coast (Eaton & Moore, 2010), which can lead to a higher compound flooding hazard associated with Q/TWL.

4.2. Compound Flood Hazard Analysis

- Joint return periods of compound flood drivers

The trivariate JRPs corresponding to the AND, OR, and Kendall scenarios are determined based on the selected marginal distributions and pair-copula functions that form the multivariate joint distributions. Results are compared with the JRPs estimated assuming that the drivers are independent to investigate the extent of under- or over-estimations of the associated hazards. At each location, the trivariate joint distribution is developed considering both conditional and unconditional pair-copulas. In trivariate analysis, the estimated JRPs are affected by the interdependencies between (Pr, Q), (Q, TWL), and (Pr, TWL).

Figure 5 shows the estimated RPs of (Pr, Q, and TWL) for univariate, independent, and OR scenarios at 41 locations across Canada's coasts considering an exceedance probability of 0.01. The median OR-JRPs and the range

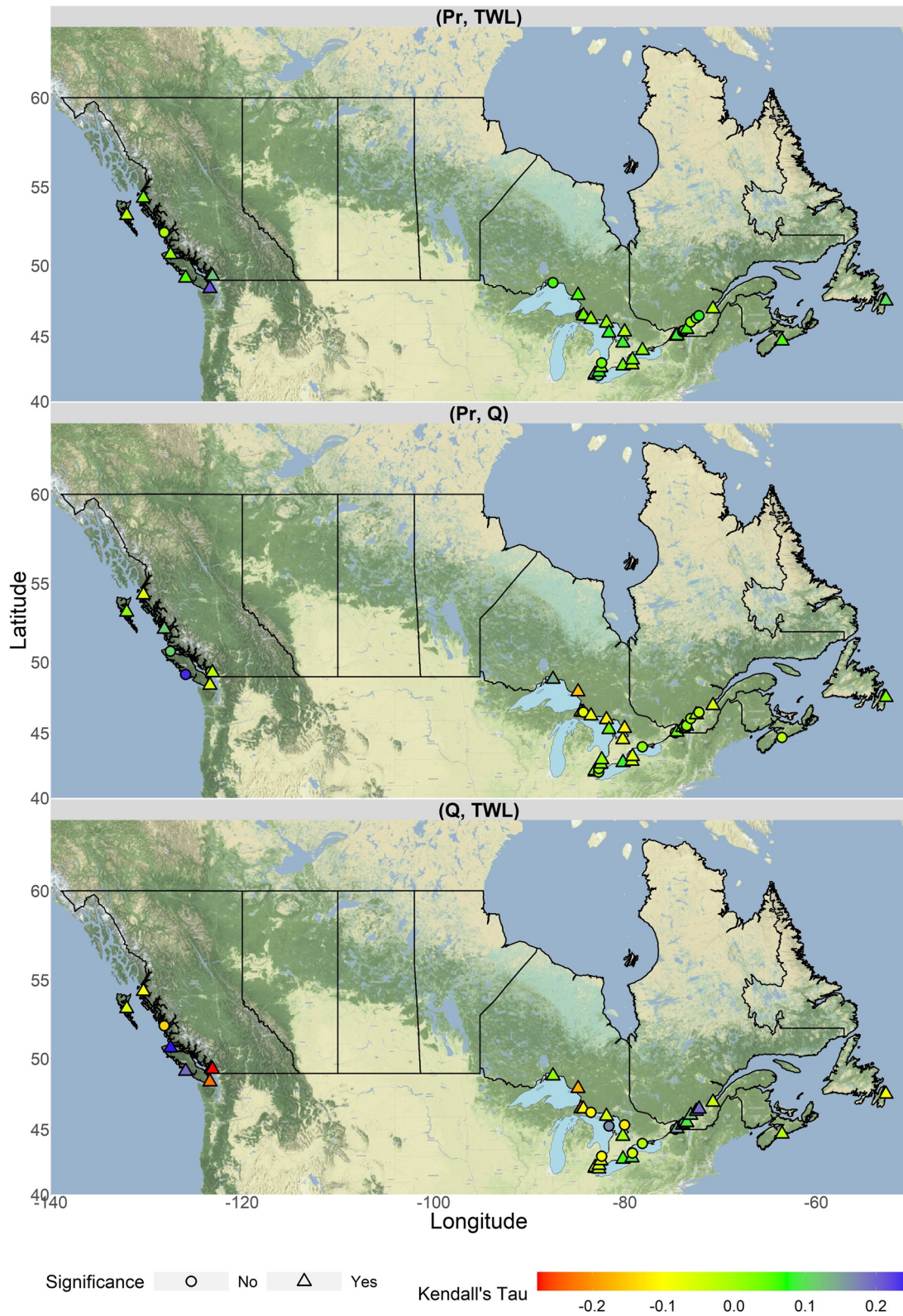


Figure 4. Kendall's Tau and its significance corresponding to (Pr, TWL), (Pr, Q), and (Q, TWL) at 41 locations across Canada.

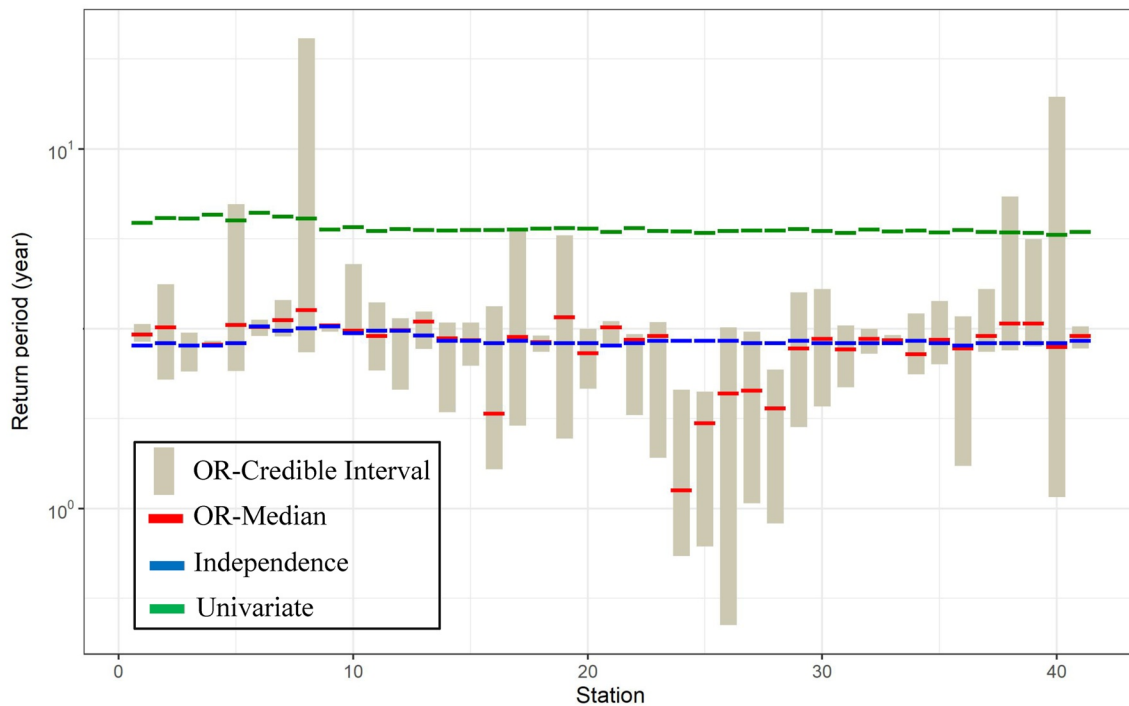


Figure 5. The estimated return periods of Pr, Q, and TWL based on univariate, independence, and OR scenarios at 41 locations across Canada's coasts.

of the uncertainties vary from 1.1 to 3.5 years and 0.08–17.5 years, respectively between all the locations. The independence OR-JRP varies from 2.8 to 3.2 years, and the univariate RPs range from 5.7 years at the Atlantic coast to 6.6 years at the Pacific coast. Overall, the estimated RPs corresponding to the univariate scenario is larger than those associated with the OR and independence scenarios. The independence and OR scenarios show larger differences at locations 24 to 29, at the Great Lakes region. The slight variations in independence and univariate cases at different locations are associated with changes in interarrival times due to different lengths of the time series. The lower bounds of the JRPs are lower than the ones based on the independence assumption, across all locations.

These differences highlight the importance of assessing multiple drivers of flooding and their interrelationships rather than studying each driver in isolation, to avoid underestimation/overestimation of the corresponding flood hazards, especially at the Great Lakes and the Atlantic coasts.

The effects of positive interrelationships between the drivers on the AND-JRPs are shown in Figure 6. In assessing this scenario, we focus on the locations where at least two out of three dependencies between the drivers are positive because if the overall dependency between the flooding drivers is negative, then, there is a rare chance of their joint occurrences. The results are compared with univariate and independent scenarios at 21 locations. JRP increase by 2% to over 15% indicating possible overestimations of compound flood hazards associated with the three drivers, in the unrealistic independence scenario, when the dependencies are negative.

The median AND-JRPs vary from 16 to 202 years between different locations which in comparison with the independence scenario changing from 58,297 to 63,879 years are remarkably lower. The range of uncertainty varies from 13 (at the Great Lakes region) to 555 years (Pacific region). The large range of uncertainty for the AND scenario is partly associated with sensitivities to the dependencies between multiple variables and the lengths of the data records. The lower quantiles in the AND-JRP are associated with higher dependencies between the drivers. The AND scenario also indicates that not considering the dependencies between the drivers can lead to underestimations of the flooding hazard (Figure 6).

It should also be mentioned that at locations 9, 12, 18 at the GL and 40 at the Atlantic area, the higher quantile JRP exceeds the independence JRP because the range of parameters for at least one pair-copula includes both negative and positive dependencies.

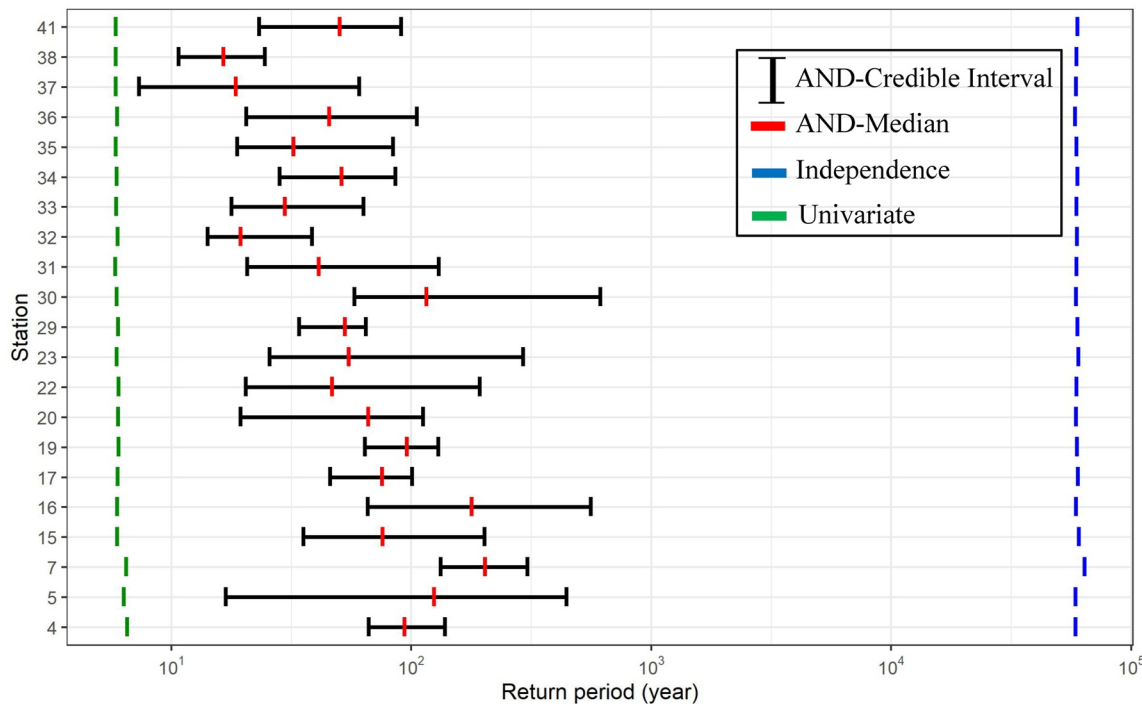


Figure 6. The estimated return periods of Pr, Q, and TWL based on univariate, independence, and AND scenarios at 21 locations across Canada's coasts.

The 100-year return period of Q under the independence condition is compared with its conditional RP considering the dependencies between the drivers. This RP is more than 100 years for 25 locations. Considering the median RP values, the maximum value is 140 years (related to higher dependency between the drivers) at location number 4 (Atlantic region) and the lowest is 89 years (related to lower dependency between the drivers) at location 24 (GL) (Figure 7). The range of the uncertainty varies from 0.4 years to more than 54 years both at the Great Lakes. These results highlight that the univariate analyses, that do not consider the interrelationships between the drivers, can lead to either under- or over-estimations of the flood hazards undermining the sustainable, long-lasting, and cost-effective engineering designs in these areas.

The results of the Kendall JRP are shown in Figure 8, which fall between the OR and AND JRPs consistent with previous studies (e.g., Xu, Wang, et al., 2019). The same is almost true for both upper and lower bounds of JRPs. Overall, the estimated minimum and maximum values are 7 (at the Great Lakes) and 662 years (Atlantic region), respectively, and the uncertainties range from 9 to 502 years across all locations. The overall comparison of the three regions shows the JRPs for the Great Lakes are lower than those of the two coastal regions, and for the Atlantic region lower than the Pacific region. Similar to the AND scenario, with an increase in the strength of the positive dependency between the drivers, the JRP decreases and vice versa. For example, if the joint events of (TWL, Pr) and (Pr, Q) show moderate positive dependencies while the (TWL, Q) event has a high negative dependency at a location, the AND and Kendall JRPs may increase. This behavior is observed at some locations such as 4 and 5 (Pacific coast), 17, 20, 22, and 29 to 38 (Great Lakes), and 41 (at Atlantic coast).

The results of the CHR index for 100-year streamflow events at 41 locations across Canada's coasts are shown in Figure 9. At 23 locations, the median index exceeds one which indicates that fluvial flood hazard is amplified by other mechanisms such as extreme sea level in the study area. These sites are highlighted in Table S3 in Supporting Information S1.

- Failure probability

We estimate the FPs corresponding to 100 and 10-year events for different hazard scenarios including OR, AND, and Kendall, and characterize their uncertainties. These FPs are compared with the estimated FPs corresponding to the independent, univariate and conditional scenarios. Analyses are conducted at all locations, however, for the sake of brevity, we present the results for location 41 at the Atlantic coast. As expected, an increase in the JRP

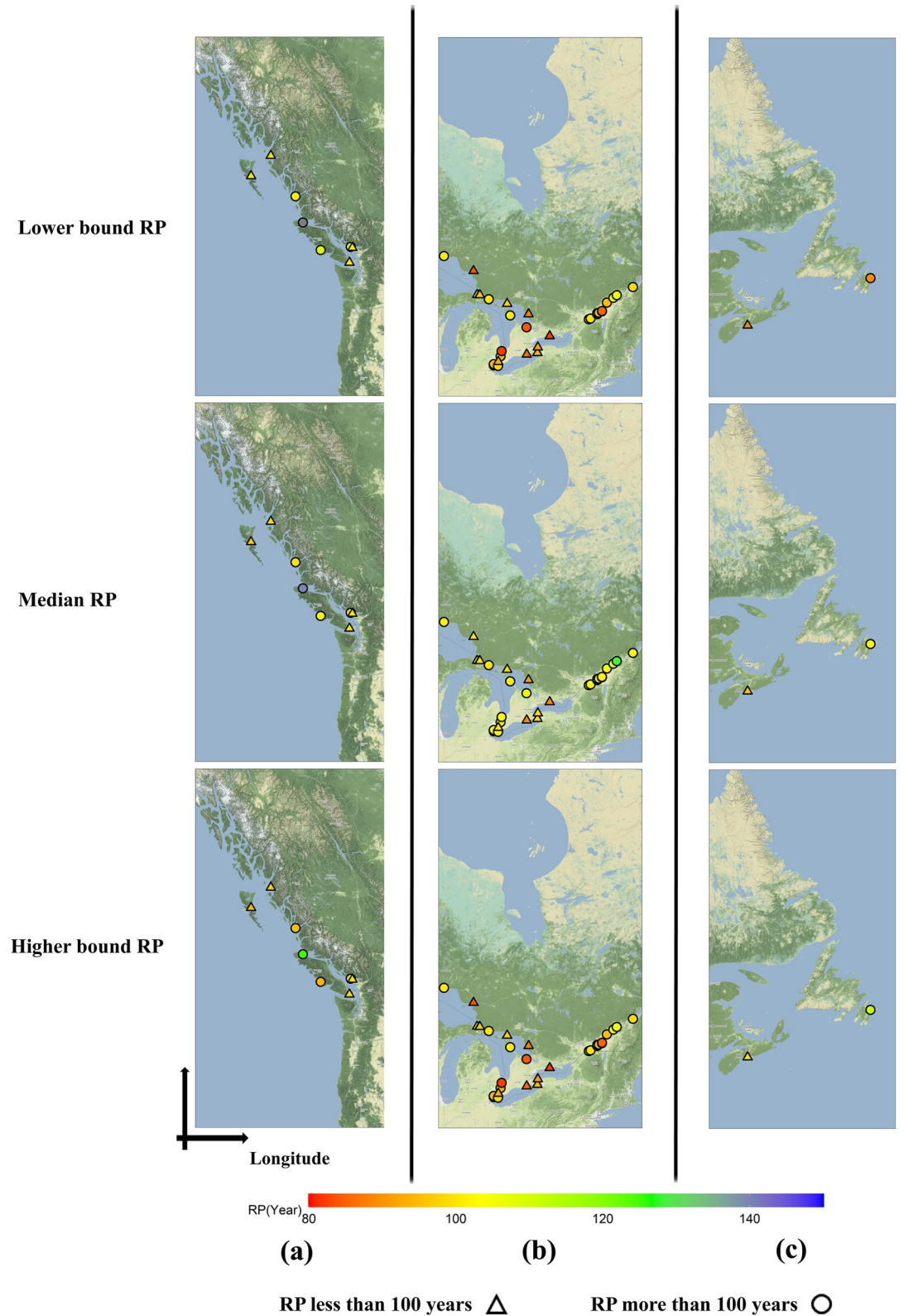


Figure 7. The return periods of Q and the corresponding uncertainties conditional on Pr and TWL for different locations across the three regions. (a) The Pacific coast (b) the Great Lakes, and (c) the Atlantic coast. The points with RPs of more and less than 100 years are shown by circles and triangles, respectively.

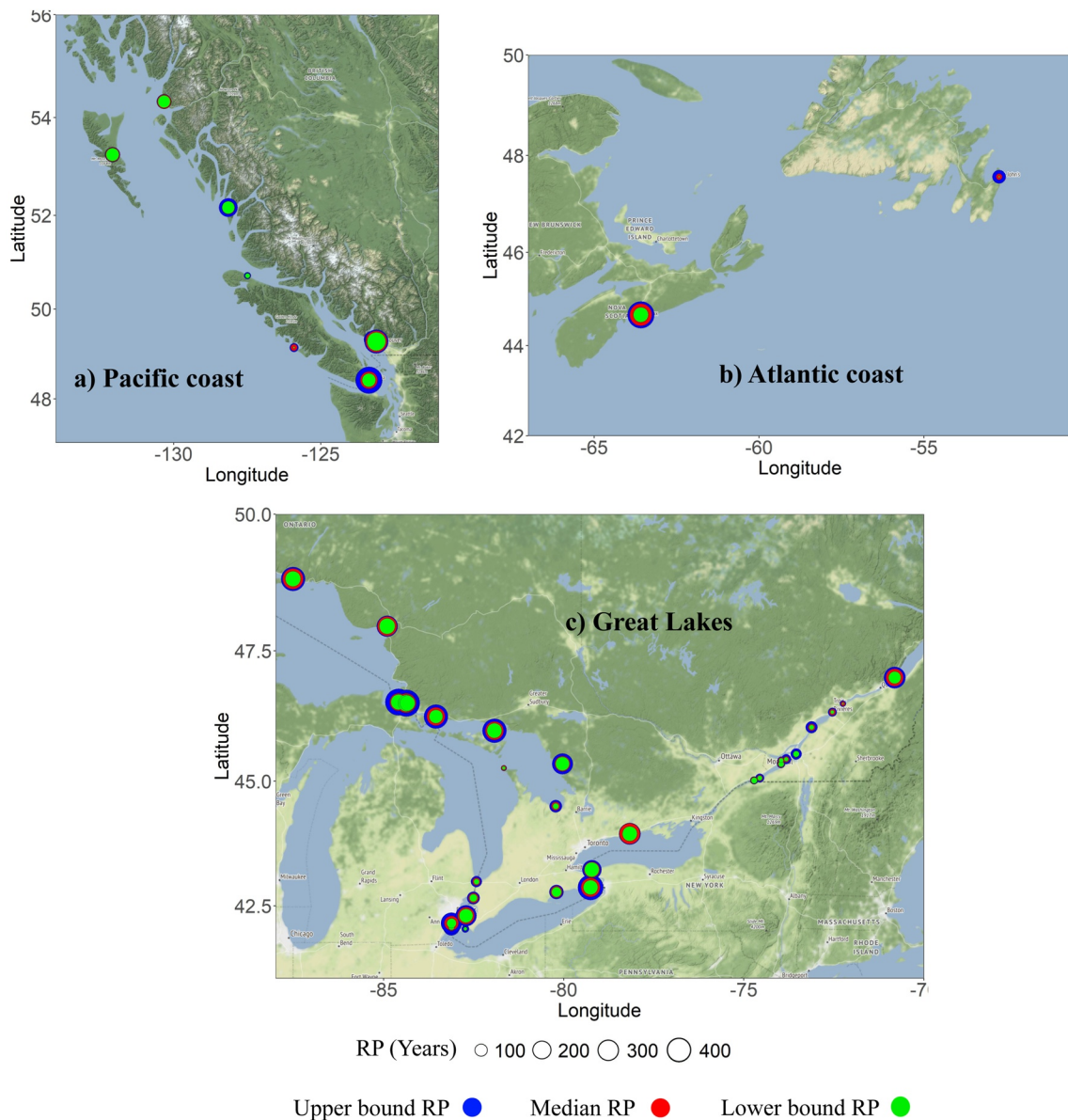


Figure 8. The estimated Kendall JRP and its uncertainty (lower and higher bounds of JRP) at different locations across three regions.

reduces the chances of the concurrent and univariate occurrence of multiple flood events and the corresponding FP values (Figure 10). These are true for three OR, AND, and Kendall scenarios, their lower quantile, and upper quantile FP values as well. Considering both RPs, the univariate and conditional univariate FP is lower than the FP of the trivariate OR scenario. This highlights the importance of analyzing the combination of multiple flood hazards at a location to avoid underestimation of the corresponding hazards. This is also evident in the univariate analysis as the conditional scenario has higher FP than the univariate scenario. Besides, under the OR scenario, the FP can be overestimated based on the independence scenario, which is consistent with studies in other areas (Moftakhari et al., 2017; Xu, Wang, et al., 2019). It should also be mentioned that under all scenarios, the FP rises with increases in the project lifetime.

The trivariate hydrologic risks (determined based on FPs) of different levels of each driver with a 100-year recurrence interval of the other two drivers are obtained for all the locations for project lifetimes of 100, 50, 20, and 5 years Figure 11 compares different scenarios for location #41 on the Atlantic coast. Accordingly, considering the median FP, the trivariate hydrologic risk is constant as long as the design rainfall is less than 80, 100, 115,

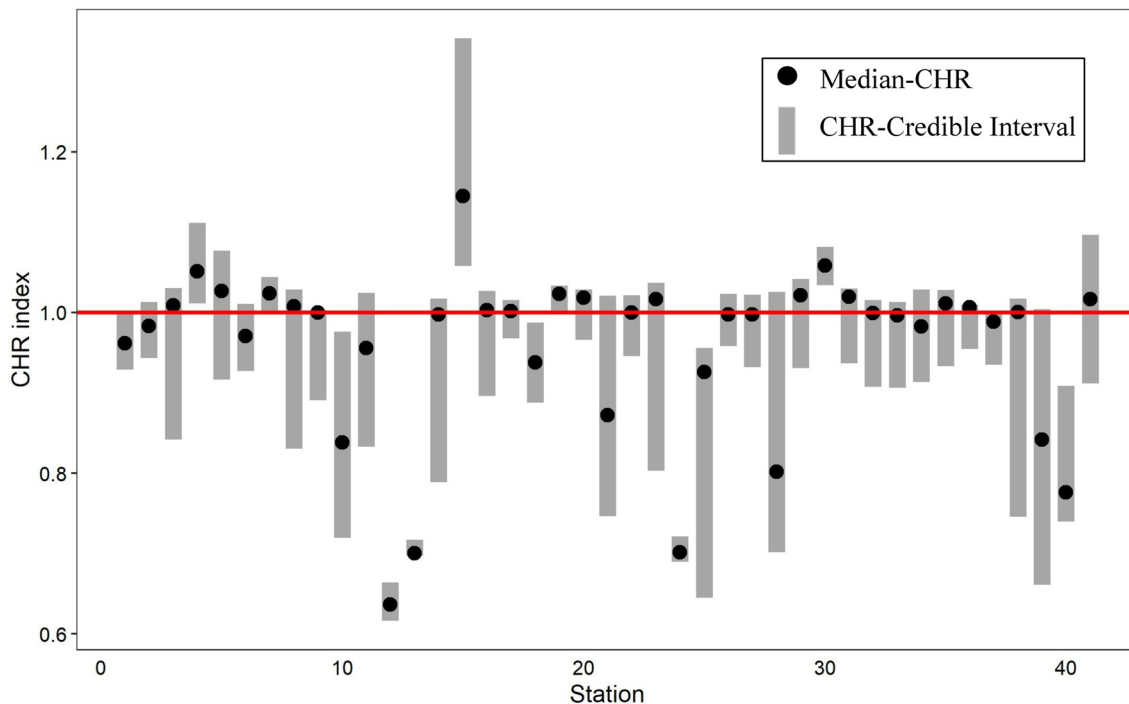


Figure 9. The CHR index and the related uncertainty estimated for Q|TWL, Pr at different locations.

and 125 mm, respectively for service times of 5, 20, 50, and 100 years and then it decreases sharply, considering 100-year Q and TWL. These values are 18, 24, 28, and 31 m³/s for design Q with 100-year Pr and TWL and 2.2, 2.4, 2.5, and 2.6 m for design TWL, with 100-year Q and Pr events. Considering the 100-year lifetime, the hydrologic risk approaches zero when the precipitation design level exceeds 170 mm and this avoids over-design leading to extra expenses. Therefore, the design rainfall in this location should be between 80 and 170 mm considering the security point of view. These design values should be between 20 and 50 m³ for Q and between 2.2 and 2.7 m for TWL. These results are important for the robust management of the coastal areas as they provide reliable hazard assessments for the engineers and the policymakers to avoid underestimation (which causes the failure of the design) or overestimation (which causes the surplus expenses) of the engineering safety levels in these areas.

The obtained results indicate that the conventional approach for flood hazard estimation, as currently adopted by most agencies, can lead to an underestimation of the corresponding risks across Canada's coastal areas in particular the Atlantic. More robust design levels are obtained by considering all the flooding mechanisms and the corresponding interrelationships. The trivariate approach proposed in this study can be applied for such analyses and other interrelated hazards.

5. Conclusions

This study analyzes the compound flood hazard hazards across Canada's coasts considering the interrelationships between three main drivers of flooding including precipitation, total water level, and streamflow. We focus on extreme precipitation events and the corresponding high flows and total water levels within a 1-day time lag. After preprocessing the data, 41 locations distributed across three regions of the Pacific, Great Lake, and Atlantic coasts are selected for the analysis of compound flooding by developing the corresponding trivariate joint distributions.

The best-fitted marginal distribution for each variable at each location is selected from 10 continuous univariate distributions. Further, according to the C-vine algorithm, the best-fitted conditional and unconditional bivariate copulas among 40 different copula functions are selected using AIC to represent the dependencies between drivers of flooding. All parameters and the corresponding uncertainties are estimated through the Bayesian approach.

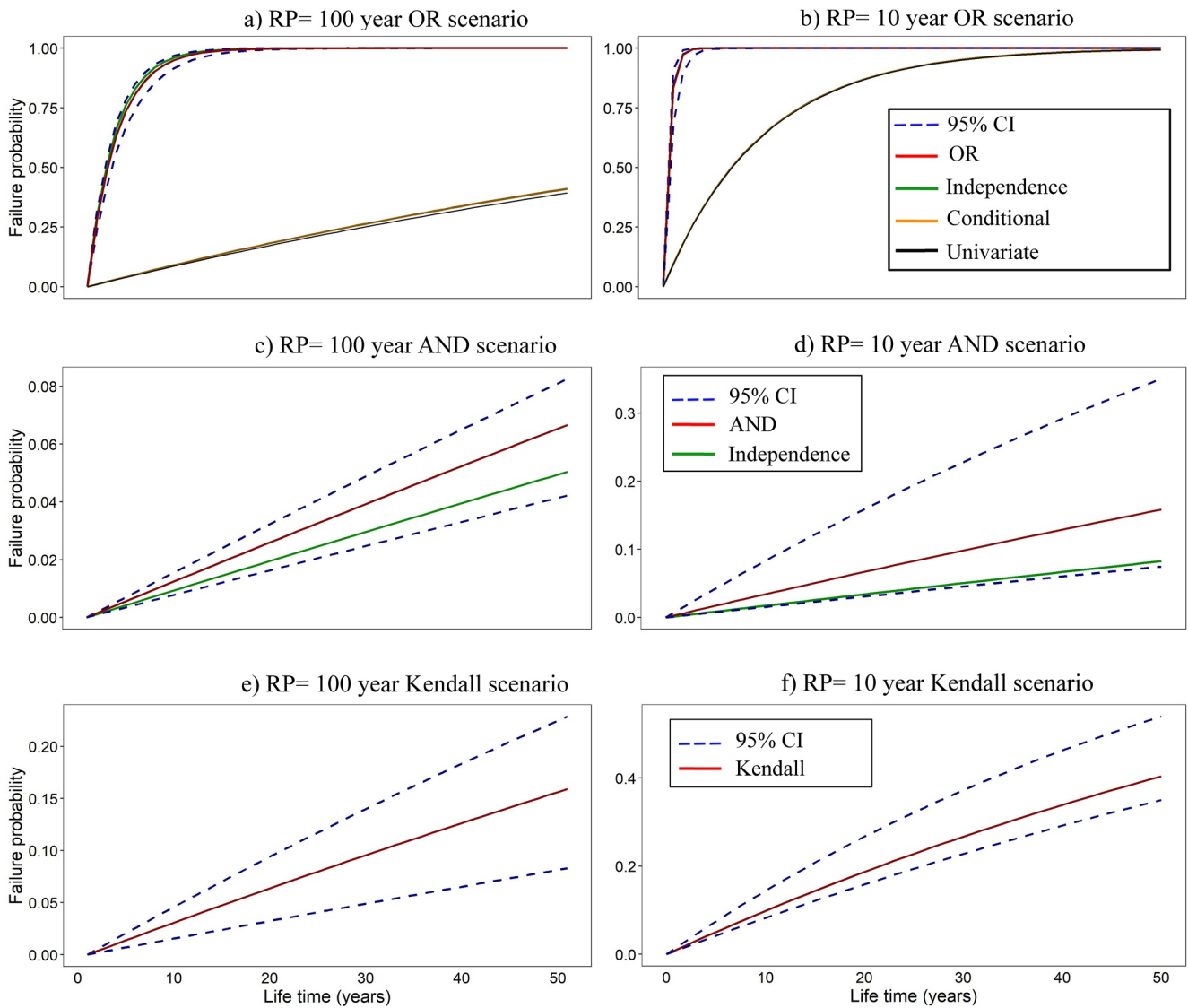


Figure 10. The failure probability (FP) values corresponding to (a, b) OR, univariate and conditional, (c, d) AND, (e, f) Kendall scenarios for 10 and 100-year events.

Further, the joint (OR, AND, Kendall) and conditional RPs and the corresponding uncertainties are quantified in this study. The return periods of individual drivers of flooding are compared with those estimated based on the joint and conditional scenarios. The results indicate positive interactions between at least two flooding drivers at 21 locations across three regions mainly at the Atlantic coast. Besides, the dependency between the TWL and Pr is higher than the other two scenarios, especially at the Atlantic coast. Results also highlight the underestimations of the corresponding hazards when drivers are investigated in isolation. Overall, 23 locations, across Canada's coasts, show positive dependencies between different drivers of flooding resulting in CHR values above unity.

The univariate analysis underestimates the failure probability of compound flood events. For example, at location 41, in the Atlantic, the FP is underestimated by almost 70% when the interrelationships between drivers of flooding are not considered considering a design lifetime of 50 years. Besides, the FP corresponding to the unrealistic independence scenario results in under- or over-estimations of FP compared to AND/OR scenarios. Considering the 100-year project lifetime, the trivariate hydrologic risk decreases sharply when the design Pr is larger than 80 mm, and approaches zero with a design level of 170 mm, suggesting a design rainfall magnitude of 80–170 mm for this location. The estimated design values of Q and TWL are between 20 and 50 m^3/s and between 2.2 and 2.8 m, respectively. The trivariate analysis conducted in the study can lead to more robust assess-

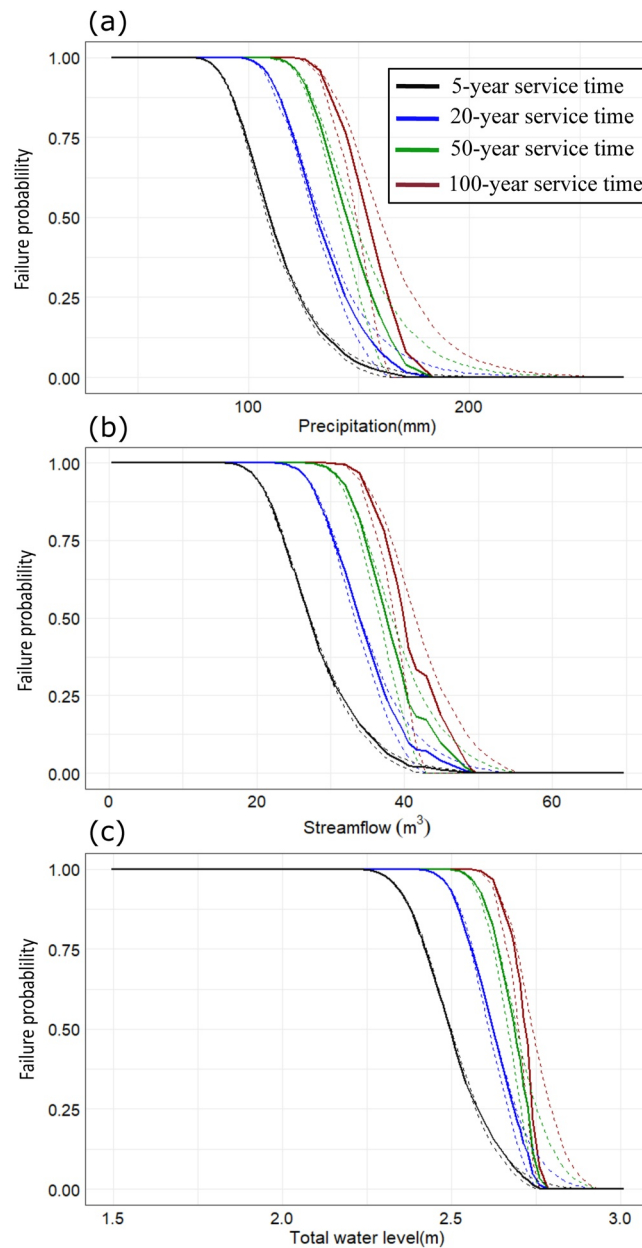


Figure 11. The trivariate hydrologic risk under different project lifetimes for each driver considering the 100-year event of the other two drivers: (a) Pr, (b) Q, and (c) TWL.

ments of the flooding hazards over the Canadian coastal zones. Further, it provides critical information for the sustainable design and planning of communities and infrastructure systems. Similar analyses can be conducted over other coastal areas.

Data Availability Statement

The hourly TWL data is available from the tidal gauge records provided by the Fisheries and Oceans Canada (<https://www.meds-sdmm.dfo-mpo.gc.ca/isdm-gdsi/twl-mne/inventory-inventaire/index-eng.htm>). To download this data type, select one of the four main regions including Pacific, Central and Arctic, Quebec, and Atlantic provided in the link above, and then click on the tidal data corresponding to each gauge which guides you to a

download link. Afterward, select the start and the end date of the data you want to download and click on the “submit” button. If any data is available in this time range, it can be downloaded. The streamflow data can be downloaded using the “ECCCDDataExplorer” software. You can narrow down your search for the gauges with specific characteristics using the options such as station number or station name, Hyd status, etc. When the gauge is selected, using the export tab >> Export selected stations, the streamflow time series can be saved. Moreover, the software provides the location of all the hydrometric gauges on a map. Daily precipitation can be obtained from the Adjusted and Homogenized Canadian Climate Data (AHCCD) (Mekis & Vincent, 2011). The Vine-Copula package (Schepsmeier et al., 2015) available in R programming software is applied to construct the pair copulas.

Acknowledgments

This project was funded by an NSERC Alliance grant in collaboration with the Institute for Catastrophic Loss Reduction (ICLR).

References

- Aas, K., & Berg, D. (2009). Models for construction of multivariate dependence—a comparison study. *The European Journal of Finance*, 15(7–8), 639–659. <https://doi.org/10.1080/13518470802588767>
- Aas, K., Czado, C., Frigessi, A., & Bakken, H. (2009). Pair-copula constructions of multiple dependence. *Insurance: Mathematics and Economics*, 44(2), 182–198. <https://doi.org/10.1016/j.insmatheco.2007.02.001>
- AghaKouchak, A., Chiang, F., Huning, L. S., Love, C. A., Mallakpour, I., Mazdiyasi, O., et al. (2020). Climate extremes and compound hazards in a warming world. *Annual Review of Earth and Planetary Sciences*, 48, 519–548. <https://doi.org/10.1146/annurev-earth-071719-055228>
- Akaike, H. (1974). A new look at the statistical model identification. *IEEE Transactions on Automatic Control*, 19(6), 716–723. <https://doi.org/10.1109/tac.1974.1100705>
- Bedford, T., & Cooke, R. M. (2001). Probability density decomposition for conditionally dependent random variables modeled by vines. *Annals of Mathematics and Artificial Intelligence*, 32(1–4), 245–268. <https://doi.org/10.1023/a:1016725902970>
- Bedford, T., & Cooke, R. M. (2002). Vines: A new graphical model for dependent random variables. *Annals of Statistics*, 1031–1068. <https://doi.org/10.1214/aos/1031689016>
- Beersma, J. J., & Buishand, T. A. (2004). Joint probability of precipitation and discharge deficits in The Netherlands. *Water Resources Research*, 40(12). <https://doi.org/10.1029/2004wr003265>
- Bevacqua, E., Maraun, D., Hobæk Haff, I., Widmann, M., & Vrac, M. (2017). Multivariate statistical modelling of compound events via pair-copula constructions: Analysis of floods in Ravenna (Italy). *Hydrology and Earth System Sciences*, 21(6), 2701–2723. <https://doi.org/10.5194/hess-21-2701-2017>
- Bevacqua, E., Voutsdoukas, M., Zappa, G., Hodges, K., Shepherd, T., Maraun, D., et al. (2020). Global projections of compound coastal meteorological extremes. <https://doi.org/10.31223/osf.io/4x2u8>
- Bevacqua, E., Voutsdoukas, M. I., Shepherd, T. G., & Vrac, M. (2020). Brief communication: The role of using precipitation or river discharge data when assessing global coastal compound flooding. *Natural Hazards and Earth System Sciences*, 20(6), 1765–1782. <https://doi.org/10.5194/nhess-20-1765-2020>
- Bezak, N., Brilly, M., & Šraj, M. (2014). Comparison between the peaks-over-threshold method and the annual maximum method for flood frequency analysis. *Hydrological Sciences Journal*, 59(5), 959–977. <https://doi.org/10.1080/02626667.2013.831174>
- Brechmann, E., & Schepsmeier, U. (2013). Cdvine: Modeling dependence with c- and d-vine copulas in R. *Journal of Statistical Software*, 52(3), 1–27. <https://doi.org/10.18637/jss.v052.i03>
- Burnham, K., Anderson, D., & Huyvaert, K. (2010). AICc model selection in ecological and behavioural science: Some background, observations and comparisons. *Behavioral Ecology and Sociobiology*, 65(1), 23–35. <https://doi.org/10.1007/s00265-010-1084-z>
- Bush, E., & Lemmen, D. (2019). *Canada's changing climate report*. Government of Canada. Government of Canada. Retrieved from <http://www.changingclimate.ca>
- Chakravarty, I. M., Roy, J., & Laha, R. G. (1967). Handbook of methods of applied statistics.
- Couason, A., Eilander, D., Muis, S., Veldkamp, T. I., Haigh, I. D., Wahl, T., et al. (2019). Measuring compound flood potential from river discharge and storm surge extremes at the global scale and its implications for flood hazard.
- Couason, A., Sebastian, A., & Morales-Nápoles, O. (2018). A copula-based Bayesian network for modeling compound flood hazard from riverine and coastal interactions at the catchment scale: An application to the Houston Ship Channel, Texas. *Water*, 10(9), 1190. <https://doi.org/10.3390/w10091190>
- Czado, C. (2010). Pair-copula constructions of multivariate copulas. In *Copula theory and its applications* (pp. 93–109). Springer.
- De Michele, C., & Salvadori, G. (2003). A generalized Pareto intensity-duration model of storm rainfall exploiting 2-copulas. *Journal of Geophysical Research*, 108(D2). <https://doi.org/10.1029/2002JD002534>
- Do, H. X., Zhao, F., Westra, S., Leonard, M., Gudmundsson, L., Boulange, J. E. S., et al. (2020). Historical and future changes in global flood magnitude—evidence from a model–observation investigation. *Hydrology and Earth System Sciences*, 24(3), 1543–1564. <https://doi.org/10.5194/hess-24-1543-2020>
- Dodangeh, E., Shahedi, K., Solaimani, K., Shiau, J.-T., & Abraham, J. (2019). Data-based bivariate uncertainty assessment of extreme rainfall-runoff using copulas: Comparison between annual maximum series (AMS) and peaks over threshold (POT). *Environmental Monitoring and Assessment*, 191(2), 67. <https://doi.org/10.1007/s10661-019-7202-0>
- dos Santos Silva, R., & Lopes, H. F. (2008). Copula, marginal distributions and model selection: A Bayesian note. *Statistics and Computing*, 18(3), 313–320. <https://doi.org/10.1007/s11222-008-9058-y>
- Eaton, B., & Moore, R. (2010). Regional hydrology. *Compendium of forest hydrology and geomorphology in British Columbia*, (Vol. 1, 85–110).
- Eckstein, D., Künzel, V., & Schäfer, L. (2021). *Global climate risk index 2021. Who suffers most from extreme weather events, 2000-2019*.
- Eilander, D., Couason, A., Ikeuchi, H., Muis, S., Yamazaki, D., Winsemius, H., & Ward, P. (2020). The effect of surge on riverine flood hazard and impact in deltas globally.
- Fang, J., Wahl, T., Fang, J., Sun, X., Kong, F., & Liu, M. (2020). Compound flood potential from storm surge and heavy precipitation in coastal China. *Hydrology and Earth System Sciences Discussions*, 1–24. <https://doi.org/10.5194/hess-25-4403-2021>
- Frame, D. J., Wehner, M. F., Noy, I., & Rosier, S. M. (2020). The economic costs of Hurricane Harvey attributable to climate change. *Climatic Change*, 160(2), 271–281. <https://doi.org/10.1007/s10584-020-02692-8>

- Ganguli, P., & Merz, B. (2019). Trends in compound flooding in northwestern Europe during 1901–2014. *Geophysical Research Letters*, 46(19), 10810–10820. <https://doi.org/10.1029/2019GL084220>
- Ganguli, P., Paprotny, D., Hasan, M., Güntner, A., & Merz, B. (2020). Projected changes in compound flood hazard from riverine and coastal floods in northwestern Europe. *Earth's Future*, 8(11), e2020EF001752. <https://doi.org/10.1029/2020EF001752>
- Genest, C., & Favre, A.-C. (2007). Everything you always wanted to know about copula modeling but were afraid to ask. *Journal of Hydrologic Engineering*, 12(4), 347–368. [https://doi.org/10.1061/\(ASCE\)1084-0699\(2007\)12:4\(347\)](https://doi.org/10.1061/(ASCE)1084-0699(2007)12:4(347))
- Genest, C., Quessy, J. F., & Rémillard, B. (2006). Goodness-of-fit procedures for copula models based on the probability integral transformation. *Scandinavian Journal of Statistics*, 33(2), 337–366. <https://doi.org/10.1111/j.1467-9469.2006.00>
- Ghanbari, M., Arabi, M., Kao, S. C., Obeysekera, J., & Sweet, W. (2021). Climate change and changes in compound coastal-riverine flooding hazard along the US coasts. *Earth's Future*, 9(5), e2021EF002055. <https://doi.org/10.1029/2021EF002055>
- Golnaraghi, M., Surminski, S., Mehryar, S., Kousky, C., & Roezer, V. (2020). Building flood resilience in a changing climate.
- González-López, V. A., Piovesana, M. C., & Romano, N. (2019). Tail conditional probabilities to predict academic performance. *4Open*, 2, 18. <https://doi.org/10.1051/fopen/2019012>
- Gori, A., Lin, N., & Xi, D. (2020). Tropical cyclone compound flood hazard assessment: From investigating dependence to quantifying impacts. *Earth and Space Science Open Archive ESSOAr*. <https://doi.org/10.1002/essoar.10503696.1>
- Hao, Z., Singh, V., & Hao, F. (2018). Compound extremes in hydroclimatology: A review. *Water*, 10(6), 718. <https://doi.org/10.3390/w10060718>
- Hendry, A., Haigh, I., Nicholls, R., Winter, H., Neal, R., Wahl, T., et al. (2019). Assessing the characteristics and drivers of compound flooding events around the UK coast. *Hydrology and Earth System Sciences*, 23, 3117–3139. <https://doi.org/10.5194/hess-23-3117-2019>
- Jalili Pirani, F., & Najafi, M. (2020). Recent trends in individual and multivariate compound flood drivers in Canada's coasts. *Water Resources Research*, 56(8), e2020WR027785. <https://doi.org/10.1029/2020WR027785>
- Jane, R., Cadavid, L., Obeysekera, J., & Wahl, T. (2020). Multivariate statistical modelling of the drivers of compound flood events in south Florida. *Natural Hazards and Earth System Sciences*, 20(10), 2681–2699. <https://doi.org/10.5194/nhess-20-2681-2020>
- Joe, H. (1996). *Families of m-variate distributions with given margins and m (m-1)/2 bivariate dependence parameters* (pp. 120–141). Lecture Notes-Monograph Series.
- Joe, H. (1997). *Multivariate models and multivariate dependence concepts*. CRC Press.
- Johnson, D. L. (2006). *Service assessment: Hurricane Katrina, August 23–31, 2005*. Silver Spring. US Department of Commerce, National Oceanic and Atmospheric Administration, & National Weather Service.
- Kundzewicz, Z. W., Kanae, S., Seneviratne, S. I., Handmer, J., Nicholls, N., Peduzzi, P., et al. (2014). Flood risk and climate change: Global and regional perspectives. *Hydrological Sciences Journal*, 59(1), 1–28. <https://doi.org/10.1080/02626667.2013.857411>
- Liu, Z., Cheng, L., Hao, Z., Li, J., Thorstensen, A., & Gao, H. (2018). A framework for exploring joint effects of conditional factors on compound floods. *Water Resources Research*, 54(4), 2681–2696. <https://doi.org/10.1002/2017WR021662>
- Mahmoudi, M. H., Najafi, M. R., Singh, H., & Schnorbus, M. (2021). Spatial and temporal changes in climate extremes over northwestern North America: The influence of internal climate variability and external forcing. *Climatic Change*, 165(1), 1–9. <https://doi.org/10.1007/s10584-021-03037-9>
- Masson-Delmotte, V., Zhai, P., Pirani, A., Connors, S. L., Péan, C., Berger, S., et al. (2021). *Climate change 2021: The physical science basis. Contribution of Working Group I to the Sixth assessment report of the Intergovernmental Panel on climate change*. IPCC.
- Mekis, É., & Vincent, L. A. J. A.-O. (2011). An overview of the second generation adjusted daily precipitation dataset for trend analysis in Canada. *Atmosphere-Ocean*, 49(2), 163–177. <https://doi.org/10.1080/07055900.2011.583910>
- Min, A., & Czado, C. (2011). Bayesian model selection for D-vine pair-copula constructions. *Canadian Journal of Statistics*, 39(2), 239–258. <https://doi.org/10.1002/cjs.10098>
- Moftakhari, H. R., Salvadori, G., AghaKouchak, A., Sanders, B. F., & Matthew, R. A. (2017). Compounding effects of sea level rise and fluvial flooding. *Proceedings of the National Academy of Sciences*, 114(37), 9785–9790. <https://doi.org/10.1073/pnas.1620325114>
- Muis, S., Verlaan, M., Winsemius, H. C., Aerts, J. C., & Ward, P. J. (2016). A global reanalysis of storm surges and extreme sea levels. *Nature Communications*, 7(1), 11969. <https://doi.org/10.1038/ncomms11969>
- Najafi, M. R., Zhang, Y., & Martyn, N. (2021). A flood risk assessment framework for interdependent infrastructure systems in coastal environments. *Sustainable Cities and Society*, 64, 102516. <https://doi.org/10.1016/j.scs.2020.102516>
- Nasr, A. A., Wahl, T., Rashid, M. M., Camus, P., & Haigh, I. D. (2021). Assessing the dependence structure between oceanographic, fluvial, and pluvial flooding drivers along the United States coastline. *Hydrology and Earth System Sciences Discussions*, 1–31. <https://doi.org/10.5194/hess-25-6203-2021>
- Nelson, R. (1998). An introduction to copulas, 1999. Lecture notes in statistics.
- Neumann, B., Vafeidis, A. T., Zimmermann, J., & Nicholls, R. J. (2015). Future coastal population growth and exposure to sea-level rise and coastal flooding—a global assessment. *PLoS One*, 10(3), e0118571. <https://doi.org/10.1371/journal.pone.0118571>
- Paprotny, D., Vousdoukas, M. I., Morales-Nápoles, O., Jonkman, S. N., & Feyen, L. (2018). Compound flood potential in Europe. *Hydrology and Earth System Sciences Discussions*, 2018, 1–34. <https://doi.org/10.5194/hess-2018-132>
- Paprotny, D., Vousdoukas, M. I., Morales-Nápoles, O., Jonkman, S. N., & Feyen, L. (2020). Pan-European hydrodynamic models and their ability to identify compound floods. *Natural Hazards*, 101(3), 933–957. <https://doi.org/10.1007/s11069-020-03902-3>
- Pitt, M., Chan, D., & Kohn, R. (2006). Efficient Bayesian inference for Gaussian copula regression models. *Biometrika*, 93(3), 537–554. <https://doi.org/10.1093/biomet/93.3.537>
- Rana, A., Moradkhani, H., & Qin, Y. (2017). Understanding the joint behavior of temperature and precipitation for climate change impact studies. *Theoretical and Applied Climatology*, 129(1), 321–339. <https://doi.org/10.1007/s00704-016-1774-1>
- Robins, P. E., Lewis, M. J., Elnahrawi, M., Lyddon, C., Dickson, N., & Coulthard, T. J. (2021). Compound flooding: Dependence at sub-daily scales between extreme storm surge and fluvial flow. *Frontiers in Built Environment*, 116. <https://doi.org/10.3389/fbuil.2021.727294>
- Salvadori, G., & De Michele, C. (2004). Frequency analysis via copulas: Theoretical aspects and applications to hydrological events. *Water Resources Research*, 40(12). <https://doi.org/10.1029/2004WR003133>
- Salvadori, G., & De Michele, C. (2010). Multivariate multiparameter extreme value models and return periods: A copula approach. *Water Resources Research*, 46(10). <https://doi.org/10.1029/2009WR009040>
- Salvadori, G., De Michele, C., Kottegoda, N. T., & Rosso, R. (2007). *Extremes in nature: An approach using copulas* (Vol. 56). Springer Science & Business Media.
- Salvadori, G., Durante, F., De Michele, C., Bernardi, M., & Petrella, L. (2016). A multivariate copula-based framework for dealing with hazard scenarios and failure probabilities. *Water Resources Research*, 52(5), 3701–3721. <https://doi.org/10.1002/2015WR017225>
- Salvadori, G., Michele, C. D., & Durante, F. (2011). On the return period and design in a multivariate framework. *Hydrology and Earth System Sciences*, 15(11), 3293–3305. <https://doi.org/10.5194/hess-15-3293-2011>

- Santos, V. M., Casas-Prat, M., Poschod, B., Ragno, E., van den Hurk, B., Hao, Z., et al. (2020). Multivariate statistical modelling of extreme coastal water levels and the effect of climate variability: A case study in The Netherlands. *Hydrology and Earth System Sciences Discussions*, 1–25. <https://doi.org/10.5194/hess-2020-536>
- Sarhadi, A., Burn, D. H., Concepcion Ausin, M., & Wiper, M. P. (2016). Time-varying nonstationary multivariate risk analysis using a dynamic Bayesian copula. *Water Resources Research*, 52(3), 2327–2349. <https://doi.org/10.1002/2015WR018525>
- Schepsmeier, U., Stoeber, J., Brechmann, E. C., Graeler, B., Nagler, T., Erhardt, T., et al. (2015). Package 'VineCopula'. R package version, 2(5).
- Sebastian, A., Dupuits, E., & Morales-Nápoles, O. (2017). Applying a Bayesian network based on Gaussian copulas to model the hydraulic boundary conditions for hurricane flood risk analysis in a coastal watershed. *Coastal Engineering*, 125, 42–50. <https://doi.org/10.1016/j.coastaleng.2017.03.008>
- Shiau, J. (2006). Fitting drought duration and severity with two-dimensional copulas. *Water Resources Management*, 20(5), 795–815. <https://doi.org/10.1007/s11269-005-9008-9>
- Singh, H., Najafi, M. R., & Cannon, A. (2022). Evaluation and joint projection of temperature and precipitation extremes across Canada based on hierarchical Bayesian modelling and large ensembles of regional climate simulations. *Weather and Climate Extremes*, 36, 100443. <https://doi.org/10.1016/j.wace.2022.100443>
- Singh, H., Najafi, M. R., & Cannon, A. J. (2021). Characterizing non-stationary compound extreme events in a changing climate based on large-ensemble climate simulations. *Climate Dynamics*, 56(5), 1389–1405. <https://doi.org/10.1007/s00382-020-05538-2>
- Singh, H., Pirani, F. J., & Najafi, M. R. (2020). Characterizing the temperature and precipitation covariability over Canada. *Theoretical and Applied Climatology*, 139(3), 1543–1558. <https://doi.org/10.1007/s00704-019-03062-w>
- Sklar, M. (1959). Fonctions de repartition an dimensions et leurs marges (Vol. 8, pp. 229–231). Publ. inst. statist. univ. Paris.
- Smith, M. S. (2011). Bayesian approaches to copula modelling. arXiv preprint arXiv:1112.4204.
- Svensson, C., & Jones, D. A. (2002). Dependence between extreme sea surge, river flow and precipitation in eastern Britain. *International Journal of Climatology: A Journal of the Royal Meteorological Society*, 22(10), 1149–1168. <https://doi.org/10.1002/joc.794>
- Tanoue, M., Hirabayashi, Y., & Ikeuchi, H. (2016). Global-scale river flood vulnerability in the last 50 years. *Scientific Reports*, 6(1), 1–9. <https://doi.org/10.1038/srep36021>
- Valle-Levinson, A., Olabarrieta, M., & Heilman, L. (2020). Compound flooding in Houston-Galveston Bay during hurricane Harvey. *Science of The Total Environment*, 747, 141272. <https://doi.org/10.1016/j.scitotenv.2020.141272>
- van Berchum, E. C., van Ledden, M., Timmermans, J. S., Kwakkel, J. H., & Jonkman, S. N. (2020). Rapid flood risk screening model for compound flood events in Beira, Mozambique. *Natural Hazards and Earth System Sciences*, 20(10), 2633–2646. <https://doi.org/10.5194/nhess-20-2633-2020>
- Villarini, G., Smith, J. A., Ntelekos, A. A., & Schwarz, U. (2011). Annual maximum and peaks-over-threshold analyses of daily rainfall accumulations for Austria. *Journal of Geophysical Research*, 116(D5). <https://doi.org/10.1029/2010JD015038>
- Wahl, T., Jain, S., Bender, J., Meyers, S. D., & Luther, M. E. (2015). Increasing risk of compound flooding from storm surge and rainfall for major US cities. *Nature Climate Change*, 5(12), 1093–1097. <https://doi.org/10.1038/nclimate2736>
- Wallemacq, P. (2018). *Economic losses, poverty & disasters: 1998-2017: Centre for Research on the Epidemiology of disasters*. CRED.
- Wang, S., Najafi, M. R., Cannon, A. J., & Khan, A. A. (2021). Uncertainties in riverine and coastal flood impacts under climate change. *Water*, 13(13), 1774. <https://doi.org/10.3390/w13131774>
- Ward, P. J., Cousnon, A., Eilander, D., Haigh, I. D., Hendry, A., Muis, S., et al. (2018). Dependence between high sea-level and high river discharge increases flood hazard in global deltas and estuaries. *Environmental Research Letters*, 13(8), 084012. <https://doi.org/10.1088/1748-9326/aad400>
- Welch, E. D. (2020). *The occurrence of compound events in Rhode Island and their associated damage costs*. University of Massachusetts Boston.
- Wu, W., McInnes, K., O'grady, J., Hoeko, R., Leonard, M., & Westra, S. (2018). Mapping dependence between extreme rainfall and storm surge. *Journal of Geophysical Research: Oceans*, 123(4), 2461–2474. <https://doi.org/10.1002/2017JC013472>
- Xu, H., Xu, K., Lian, J., & Ma, C. (2019). Compound effects of rainfall and storm tides on coastal flooding risk. *Stochastic Environmental Research and Risk Assessment*, 33(7), 1249–1261. <https://doi.org/10.1007/s00477-019-01695-x>
- Xu, K., Ma, C., Lian, J., & Bin, L. (2014). Joint probability analysis of extreme precipitation and storm tide in a coastal city under changing environment. *PLoS One*, 9(10), e109341. <https://doi.org/10.1371/journal.pone.0109341>
- Xu, P., Wang, D., Singh, V. P., Wang, Y., Wu, J., Lu, H., et al. (2019). Time-varying copula and design life level-based nonstationary risk analysis of extreme rainfall events. *Hydrology and Earth System Sciences Discussions*, 1–59. <https://doi.org/10.5194/hess-2019-358>
- Zhang, Y., & Najafi, M. R. (2020). Probabilistic numerical modeling of compound flooding caused by tropical storm Matthew over a data-scarce coastal environment. *Water Resources Research*, 56(10), e2020WR028565. <https://doi.org/10.1029/2020WR028565>
- Zheng, F., Westra, S., Leonard, M., & Sisson, S. A. (2014). Modeling dependence between extreme rainfall and storm surge to estimate coastal flooding risk. *Water Resources Research*, 50(3), 2050–2071. <https://doi.org/10.1002/2013WR014616>
- Zheng, F., Westra, S., & Sisson, S. A. (2013). Quantifying the dependence between extreme rainfall and storm surge in the coastal zone. *Journal of Hydrology*, 505, 172–187. <https://doi.org/10.1016/j.jhydrol.2013.09.054>
- Zscheischler, J., Westra, S., Van Den Hurk, B. J., Seneviratne, S. I., Ward, P. J., Pitman, A., et al. (2018). Future climate risk from compound events. *Nature Climate Change*, 8(6), 469–477. [10.1038/s41558-018-0156-3](https://doi.org/10.1038/s41558-018-0156-3)

References From the Supporting Information

- Genest, C., & Rivest, L.-P. (1993). Statistical inference procedures for bivariate Archimedean copulas. *Journal of the American Statistical Association*, 88(423), 1034–1043. <https://doi.org/10.2307/2290796>
- Geweke, J. (1991). *Evaluating the accuracy of sampling-based approaches to the calculation of posterior moments* (Vol. 196). Federal Reserve Bank of Minneapolis, Research Department.
- Gräler, B., van den Berg, M., Vandenberghe, S., Petroselli, A., Grimaldi, S., De Baets, B., & Verhoest, N. (2013). Multivariate return periods in hydrology: A critical and practical review focusing on synthetic design hydrograph estimation. *Hydrology and Earth System Sciences*, 17(4), 1281–1296. <https://doi.org/10.5194/hess-17-1281-2013>
- Hastings, W. K. (1970). Monte Carlo sampling methods using Markov chains and their applications.
- Wang, W., & Wells, M. T. (2000). Model selection and semiparametric inference for bivariate failure-time data. *Journal of the American Statistical Association*, 95(449), 62–72. <https://doi.org/10.1080/01621459.2000.10473899>